PHYSICAL REVIEW A **92**, 060302(R) (2015)

Characterizing universal gate sets via dihedral benchmarking

Arnaud Carignan-Dugas,[1] Joel J. Wallman,[1] and Joseph Emerson[1,2]
[1]*Institute for Quantum Computing and the Department of Applied Mathematics, University of Waterloo, Waterloo, Ontario, Canada N2L 3G1*
[2]*Canadian Institute for Advanced Research, Toronto, Ontario, Canada M5G 1Z8*
(Received 27 August 2015; published 28 December 2015)

We describe a practical experimental protocol for robustly characterizing the error rates of non-Clifford gates associated with dihedral groups, including small single-qubit rotations. Our dihedral benchmarking protocol is a generalization of randomized benchmarking that relaxes the usual unitary 2-design condition. Combining this protocol with existing randomized benchmarking schemes enables practical universal gate sets for quantum information processing to be characterized in a way that is robust against state-preparation and measurement errors. In particular, our protocol enables direct benchmarking of the $\pi/8$ gate even under the gate-dependent error model that is expected in leading approaches to fault-tolerant quantum computation.

DOI: 10.1103/PhysRevA.92.060302 PACS number(s): 03.67.Lx, 03.65.Fd, 03.65.Yz, 03.67.Ac

A universal quantum computer is a device allowing for the implementation of arbitrary unitary transformations. As with any scenario involving control, a practical quantum computation will inevitably have errors. While the complexity of quantum dynamics is what enables the unique capabilities of quantum computation, including important applications such as quantum simulation and Shor's factoring algorithm, that same complexity poses a unique challenge to efficiently characterizing the errors. One approach is quantum process tomography [1,2], which completely characterizes the errors on arbitrary quantum gates but requires resources that scale exponentially in the number of qubits. Moreover, quantum process tomography is sensitive to state-preparation and measurement (SPAM) errors [3].

Randomized benchmarking [4–7] using a unitary 2-design [8], such as the Clifford group, overcomes both of these limitations by providing an estimate of the error rate per gate averaged over the 2-design. More specifically, it is a method for efficiently estimating the average fidelity

$$\mathcal{F}_{\text{avg}}(\mathcal{E}) := \int d\psi \, \langle\psi|\mathcal{E}(\psi)|\psi\rangle \tag{1}$$

of a noise map $\mathcal{E}$ associated with any group of quantum operations forming a unitary 2-design in a way that is robust against SPAM errors. This partial information is useful in practice as it provides an efficient means of tuning up experimental performance, and, moreover, provides a bound on the threshold error rate required for fault-tolerant quantum computing [9] that becomes tight when the noise is stochastic [7,10–14].

An important limitation of existing randomized benchmarking methods is that they are only efficient in the number of qubits [4,6,8] for nonuniversal sets of gates such as the Clifford group. While Clifford gates play an important role in many fault-tolerant approaches to quantum computation [9], one still needs a means of benchmarking an additional non-Clifford gate required for universality. One approach is to separately benchmark distinct unitary 2-designs [15]. While this approach is relatively straightforward for characterizing gates at the physical level, it is unclear how to apply this approach in the context of leading fault-tolerant proposals wherein particular non-Clifford operations required for universality, such as the $\pi/8$ gate, are implemented via magic-state distillation and gate injection [16,17], which is a complex procedure that will be subject to dramatically different error rates than those of the (physical or logical) Clifford gates. Alternatively, randomized benchmarking tomography [18] can be employed, although the fast decay curves can have a large uncertainty due to fitting an exponential to a small number of significant data points.

In the present Rapid Communication, we describe a protocol for benchmarking the average fidelity of a group of operations corresponding to the dihedral group which does not satisfy the usual 2-design constraint for randomized benchmarking. However, we show that the dihedral benchmarking protocol still allows the average fidelity to be estimated while retaining many of the benefits of standard randomized benchmarking. Furthermore, by combining our dihedral benchmarking protocol with both standard [6] and interleaved randomized benchmarking [19], we give an explicit method for characterizing the average fidelity of the $\pi/8$ gate directly. This is of particular interest because the $\pi/8$ gate combined with the generators of the Clifford group [e.g., the controlled-NOT (CNOT), the Hadamard, and the Pauli gates] provides a standard gate set for generating universal quantum computation. Moreover, our protocol enables characterization of non-Clifford gates associated with small-angle rotations, which are of interest to achieve more efficient fault-tolerant circuits [20–22]. Furthermore, the dihedral benchmarking protocol can be implemented either at the physical or logical level, but will find its greatest impact in the latter case, which is relevant to fault-tolerant quantum computation via magic-state injection. In that setting, the quality of a logical $\pi/8$ gate implemented via gate injection will depend in a complex way on the quality of the input (distilled) magic state, the errors on the physical stabilizer operations, and the errors in the stabilizer measurements, all of which are required for the injection routine. Applying our protocol at the logical level provides a direct means of benchmarking the logical error rate of the injected $\pi/8$ gate, which may be dramatically different from the error rates achieved for the logical Clifford operations under the fault-tolerant encoding, without assessing the performance of the individual components. Remarkably, dihedral benchmarking overcomes the key assumption of "weak gate dependence" of the noise that limits previous benchmarking protocols. Specifically, the protocol is robust in the important setting when the error on the non-Clifford gate, such as the $\pi/8$ gate, is substantially different from

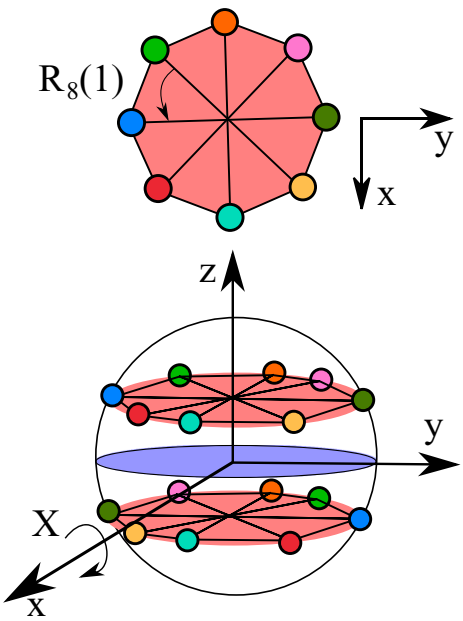

FIG. 1. (Color online) The orbit, under the action of the dihedral group $\mathcal{D}_8$, of an input state located at a 45° latitude on the Bloch sphere. $R_8(z)$ are the rotations of the octagon, while X is a reflection (or a rotation in three dimensions, with the rotation axis parallel to the octagon's surface). The $\pi/8$ gate corresponds to the smallest rotation $R_8(1)$.

the error on the Clifford operations. As noted above, this is the expected scenario in leading approaches to fault-tolerant quantum computation.

Characterizing single-qubit unitary groups. We now outline a protocol that yields the average gate fidelity of the experimental implementation of a single-qubit unitary group of the form

$$\mathcal{D}_j = \langle R_j(1), X \rangle, \tag{2}$$

where $\langle \cdots \rangle$ denotes the group generated by the arguments, j is a positive integer (or an arbitrary real number), and

$$R_j(z) := e^{\pi i z Z/j} = \cos(\pi z/j)\mathbb{I} + i \sin(\pi z/j) Z. \tag{3}$$

Up to an overall sign, $\mathcal{D}_j$ is a representation of the dihedral group of order $2j$, with $X R_j(z) = R_j(-z)X$, which is not a unitary 2-design and includes gates producing arbitrarily small rotations as j increases. Note that the choice of rotation axis is arbitrary, and that any single-qubit gate can be written as $R_j(1)$ relative to some axis. Consequently, our protocol will allow any single-qubit gate to be benchmarked. The Bloch sphere representation of $\mathcal{D}_8$ acting on a qubit state is illustrated in Fig. 1. This group contains the so-called $\pi/8$ gate, which corresponds to the $R_8(1)$ rotation.

The dihedral benchmarking protocol for a fixed integer j is as follows. (Note that j can also be a real number, in which case the sums below are replaced by integrals.)

1. Choose two strings of length m, $\mathbf{z} = (z_1, \ldots, z_m) \in \mathbb{Z}_j^m$ and $\mathbf{x} = (x_1, \ldots, x_m) \in \mathbb{Z}_2^m$, independently and uniformly at random.
2. Prepare a system in an arbitrary initial state ρ.[1]
3. At each time step $t = 1, \ldots, m$, apply $R_j(z_t)X^{x_t}$.
4. Apply the inversion gate, defined as

$$G_{\text{inv.}} := X^{b_1} Z^{b_2} \prod_{t=1}^{m} [R_j(z_t)X^{x_t}]^\dagger,$$

where $b_1, b_2 \in \mathbb{Z}_2$ are fixed by considerations below.

5. Perform a positive-operator-valued measure (POVM) $\{+1, -1\} \to \{E, \mathbb{I} - E\}$ for some $E \approx \rho$, to estimate the probability $q(+1|m, x, z, b_1, b_2)$ of outcome $+1$.
6. Repeat steps 1–5 k times, where k is fixed by the requirement to estimate the average survival probability

$$p(m, b_1, b_2) := |2j|^{-(m+1)} \sum_{x,z} q(+1|m, x, z, b_1, b_2)$$

to a desired precision (see Refs. [7,10,23] for details on the required sampling complexity).

For $b_1 = b_2 = 0$, the average survival probability is

$$p(m, 0, 0) = A\tilde{p}_0^m + B\tilde{p}_1^m + C, \tag{4}$$

where A, B, and C are constants absorbing SPAM factors. Fitting two exponentials is generally more difficult than fitting a single exponential, so we propose instead fitting to

$$p(m,0,0) + p(m,0,1) - p(m,1,0) - p(m,1,1) = 4A\tilde{p}_0^m \tag{5}$$

and

$$p(m,0,0) - p(m,0,1) = 2B\tilde{p}_1^m. \tag{6}$$

As we will show below, the average gate fidelity is related to the fit parameters $\tilde{p}_0$ and $\tilde{p}_1$ by

$$\mathcal{F}_{\text{avg}}(\mathcal{E}_{\mathcal{D}_j}) = \frac{1}{2} + \frac{1}{6}(\tilde{p}_0 + 2\tilde{p}_1), \tag{7}$$

where $\mathcal{E}_{\mathcal{D}_j}$ is the noise over $\mathcal{D}_j$ and we assume that the noise is completely positive and trace preserving and is also gate and time independent (though perturbative approaches to relax these assumptions can be considered [7,10])

Characterizing the $\pi/8$ gate. The $\pi/8$ gate, or $R_8(1)$ in the notation of Eq. (3), is important in many implementations because it is used to supplement the Clifford gates to achieve universal quantum computation. In leading approaches to fault-tolerant error correction, the $\pi/8$ gate is physically realized via magic-state injection [16], in which magic states are acted upon by Clifford transformation and postselected stabilizer measurements. Because the physical (logical) Clifford gates are applied directly (transversally) whereas the $\pi/8$ gate is implemented through the above method, the error on the $\pi/8$ gate may be substantially different and requires separate characterization. While the quality of the injected gate can be assessed by measuring the quality of the input and output magic states as well as benchmarking the required stabilizer

[1]The constants A and B appearing in Eqs. (5) and (6) depend on state preparation, as shown in Eqs. (23)–(25). These constants may be maximized by choosing an appropriate state preparation (and the corresponding measurement). In particular, optimal states for Eqs. (5) and (6) are $|0\rangle\langle 0|$ and $|+\rangle\langle +|$, respectively.

operations, here we provide a direct method to estimate the average gate fidelity of the $\pi/8$ gate.

The $\pi/8$ gate is contained in $\mathcal{D}_8$ [see Eq. (2)], which contains $\mathcal{D}_4$ as a subgroup. One approach to characterizing the $\pi/8$ gate is to benchmark $\mathcal{D}_4$ and $\mathcal{D}_8$ separately. If the average fidelities over $\mathcal{D}_8$ and $\mathcal{D}_4$ are similar, this is an indication that the $\pi/8$ gate has a similar average fidelity as the Clifford group. However, typically this will not hold for the reasons stated above, in which case we suggest the following protocol. First, benchmark $\mathcal{D}_4$ as per the above protocol. Then adapt interleaved randomized benchmarking [24] to the above protocol by replacing steps 3 and 4 (with $j = 4$) with the two following steps:

3′. At each time step $t = 1, \ldots, m$, apply $R_8(1)R_4(z_t)X^{x_t}$.

4′. Apply the inversion gate, defined as

$$G_{\text{inv}} := X^{b_1} Z^{b_2} \prod_{t=1}^{m} [R_8(1)R_4(z_t)X^{x_t}]^{\dagger}.$$

We require the sequence length to be even to ensure that the inversion gate is in $\mathcal{D}_4$, which follows from the commutation relation $XR_j(z) = R_j(-z)X$. For $b_1 = b_2 = 0$, the average survival probability is similar to Eq. (4), but with different decay parameters:

$$p(m,0,0) = A'\tilde{q}_0^m + B'\tilde{q}_1^m + C'. \tag{8}$$

As above, the curves

$$p(m,0,0) + p(m,0,1) - p(m,1,0) - p(m,1,1) = 4A'\tilde{q}_0^m \tag{9}$$

and

$$p(m,0,0) - p(m,0,1) = 2B'\tilde{q}_1^m \tag{10}$$

can be fitted instead to extract the decay parameters. The average gate fidelity of the composed noise channel $\mathcal{E}_{\pi/8} \circ \mathcal{E}_{\mathcal{D}_4}$ (where $\mathcal{E}_{\pi/8}$ is the noise on the $\pi/8$ gate and $\circ$ denotes channel composition) is related to the fit parameters $\tilde{q}_0$ and $\tilde{q}_1$ by

$$\mathcal{F}_{\text{avg}}(\mathcal{E}_{\pi/8} \circ \mathcal{E}_{\mathcal{D}_4}) = \frac{1}{2} + \frac{1}{6}(\tilde{q}_0 + 2\tilde{q}_1). \tag{11}$$

The average gate fidelity of the $\pi/8$ gate, $\mathcal{F}_{\text{avg}}(\mathcal{E}_{\pi/8})$ (as opposed to the fidelity of the composite noise channel), can then be estimated from the relation [18,25]

$$\begin{aligned} &\left|\chi_{00}^{\mathcal{E}_{\pi/8}} - \chi_{00}^{\mathcal{E}_{\mathcal{D}_4}} \chi_{00}^{\mathcal{E}_{\pi/8}\circ\mathcal{E}_{\mathcal{D}_4}} - \left(1 - \chi_{00}^{\mathcal{E}_{\mathcal{D}_4}}\right)\left(1 - \chi_{00}^{\mathcal{E}_{\pi/8}\circ\mathcal{E}_{\mathcal{D}_4}}\right)\right| \\ &\quad \leqslant 2\sqrt{\chi_{00}^{\mathcal{E}_{\mathcal{D}_4}} \chi_{00}^{\mathcal{E}_{\pi/8}\circ\mathcal{E}_{\mathcal{D}_4}} \left(1 - \chi_{00}^{\mathcal{E}_{\mathcal{D}_4}}\right)\left(1 - \chi_{00}^{\mathcal{E}_{\pi/8}\circ\mathcal{E}_{\mathcal{D}_4}}\right)}, \end{aligned} \tag{12}$$

where

$$\chi_{00}^{\mathcal{E}} = \frac{3}{2}\mathcal{F}_{\text{avg}}(\mathcal{E}) - \frac{1}{2}. \tag{13}$$

This bound is loose in general but tight when the Clifford gates in $\mathcal{D}_4$ have much higher fidelity than the $\pi/8$ gate (which is the regime of interest when optimizing the overhead and fidelity of the distillation and injection routines) [26].

Smaller rotations can also be characterized in a similar fashion. The average fidelity of a small rotation $R_J(1)$ is estimated by implementing the same scheme, replacing $\pi/8$ with $R_J(1), \mathcal{D}_4$ with $\mathcal{D}_j$ such that $2Nj = J$ for any fixed choice of $N \in \mathbb{N}$, and by restricting the sequence lengths to be multiples of $2N$.

Analysis. We now derive the formula for the decay curves expressed in Eqs. (4)–(6) and (8)–(10) together with the average fidelity Eqs. (7) and (11). For convenience, we will use the Pauli-Liouville representation of channels in which channel composition corresponds to matrix multiplication (see, e.g., Ref. [10] for details). The Pauli-Liouville representation of an abstract channel $\mathcal{E}$, which we denote with a bold font $\boldsymbol{\mathcal{E}}$, is the matrix of trace inner products between Pauli matrices P_j and their images $\mathcal{E}(P_k)$ under $\mathcal{E}$,

$$\boldsymbol{\mathcal{E}}_{jk} = \text{Tr}[P_j \mathcal{E}(P_k)]. \tag{14}$$

We assume that the experimental noise is completely positive and trace preserving and is also gate and time independent (though perturbative approaches to relax these assumptions can be considered [7,10]), so that we can represent the experimental implementation of $R_J(1)R_j(z)X^x$ as $\boldsymbol{\mathcal{R}}_J(1)\boldsymbol{\mathcal{E}}_{R_J(1)}\boldsymbol{\mathcal{E}}_{\mathcal{D}_j}\boldsymbol{\mathcal{R}}_j(z)\boldsymbol{\mathcal{X}}^x$. The standard $\mathcal{D}_j$ benchmarking protocol can be obtained by setting $J = 1$ and $\boldsymbol{\mathcal{E}}_{R_J(1)} = \mathbb{I}$, while the interleaved case corresponds to $J = 2Nj$.

For $j > 2$, the Pauli-Liouville representation of $\mathcal{D}_j$ is block diagonal with three blocks, where the blocks corresponds to three inequivalent irreducible representations (irreps) of the dihedral group, namely,

1. $R_j(z)X^x \to 1$ (trivial representation),
2. $R_j(z)X^x \to \left(\begin{smallmatrix} \cos(2\pi z/j) & (-1)^{x+1}\sin(2\pi z/j) \\ \sin(2\pi z/j) & (-1)^x \cos(2\pi z/j) \end{smallmatrix}\right)$ (faithful representation),
3. $R_j(z)X^x \to (-1)^x$ (parity representation).

This is easily seen by looking at the action of $\mathcal{D}_j$ on the Bloch sphere (see Fig. 1). The trivial representation emerges from the unitality and trace-preserving properties of unitary operations, which map any Bloch shell of constant radius to itself, including the center point. The parity representation encodes the fact that the $\pm Z$ poles of the Bloch sphere are invariant under conjugation by $R_j(z)$ and swapped under conjugation by X. The two-dimensional representation encodes the action of $R_j(z)X^x$ on the XY plane of the Bloch sphere.

The *twirl* of $\boldsymbol{\mathcal{E}}$ over a group $\mathcal{G}$ is

$$\boldsymbol{\mathcal{E}}^{\mathcal{G}} = (|\mathcal{G}|)^{-1} \sum_{\mathcal{U}\in\mathcal{G}} \boldsymbol{\mathcal{U}}^{-1}\boldsymbol{\mathcal{E}}\boldsymbol{\mathcal{U}}. \tag{15}$$

As a consequence of Schur's lemmas (see the Supplemental Material of Ref. [24]), the twirl of any channel over $\mathcal{D}_j$ is

$$\boldsymbol{\mathcal{E}}^{\mathcal{D}_j} = (\boldsymbol{\mathcal{E}}_{R_J(1)}\boldsymbol{\mathcal{E}}_{\mathcal{D}_j})^{\mathcal{D}_j} = \begin{pmatrix} 1 & 0 & 0 & 0 \\ 0 & \tilde{q}_1 & 0 & 0 \\ 0 & 0 & \tilde{q}_1 & 0 \\ 0 & 0 & 0 & \tilde{q}_0 \end{pmatrix} \tag{16}$$

for $j > 2$, where $\tilde{q}_0 := \boldsymbol{\mathcal{E}}_{44}$ and $\tilde{q}_1 := \frac{\boldsymbol{\mathcal{E}}_{22}+\boldsymbol{\mathcal{E}}_{33}}{2}$ and the diagonal blocks correspond to the three inequivalent irreps of $\mathcal{D}_j$. Defining

$$\begin{aligned} \boldsymbol{\mathcal{A}}_m &:= (2j)^{-m} \sum_{x,z} \prod_{i=m}^{1} \boldsymbol{\mathcal{R}}_J(1)\boldsymbol{\mathcal{E}}_{R_J(1)}\boldsymbol{\mathcal{E}}_{\mathcal{D}_j}\boldsymbol{\mathcal{R}}_j(z_i)\boldsymbol{\mathcal{X}}^{x_i}, \\ \boldsymbol{\mathcal{B}}_m &:= (2j)^{-m} \sum_{x,z} \prod_{i=1}^{m} \boldsymbol{\mathcal{X}}^{x_i\dagger}\boldsymbol{\mathcal{R}}_j(z_i)^{\dagger}\boldsymbol{\mathcal{R}}_J(1)^{\dagger}, \end{aligned} \tag{17}$$

the average over all sequences of length m can be expressed as the effective channel

$$\mathcal{C} = \mathcal{E}_{\mathcal{D}_j} \mathcal{X}^{b_1} \mathcal{Z}^{b_2} \mathcal{B}_m \mathcal{A}_m. \tag{18}$$

But $\mathcal{B}_m \mathcal{A}_m$ can be reexpressed as

$$\begin{aligned} \mathcal{B}_m \mathcal{A}_m &= \mathcal{B}_{m-1} \left(\mathcal{E}_{R_J(1)} \mathcal{E}_{\mathcal{D}_j}\right)^{\mathcal{D}_j} \mathcal{A}_{m-1} \\ &= \left(\mathcal{E}_{R_J(1)} \mathcal{E}_{\mathcal{D}_j}\right)^{\mathcal{D}_j} \mathcal{B}_{m-1} \mathcal{A}_{m-1} \\ &= \prod_{j=1}^{m} \left(\mathcal{E}_{R_J(1)} \mathcal{E}_{\mathcal{D}_j}\right)^{\mathcal{D}_j}, \end{aligned} \tag{19}$$

where the the second line follows from the fact that $\mathcal{E}^{\mathcal{D}_j}$ is proportional to the identity in each of the blocks.

With these definitions, the average fidelity is [18,27]

$$\begin{aligned} \mathcal{F}_{\text{avg.}}(\mathcal{E}) &= \frac{1}{2} + \frac{1}{6}(\mathcal{E}_{22} + \mathcal{E}_{33} + \mathcal{E}_{44}) \\ &= \frac{1}{2} + \frac{1}{6}(\tilde{q}_0 + 2\tilde{q}_1), \end{aligned} \tag{20}$$

as in Eqs. (7) and (11). Using Eq. (16), the effective channel $\mathcal{C}$ from Eq. (18) can readily be expressed as

$$\mathcal{C} = \mathcal{E}_{\mathcal{D}_j} \begin{pmatrix} 1 & 0 & 0 & 0 \\ 0 & (-1)^{b_2} \tilde{q}_1^m & 0 & 0 \\ 0 & 0 & (-1)^{b_1+b_2} \tilde{q}_1^m & 0 \\ 0 & 0 & 0 & (-1)^{b_1} \tilde{q}_0^m \end{pmatrix}. \tag{21}$$

Therefore the survival probability is

$$\begin{aligned} p(m,b_1,b_2) &= \text{Tr}[E\mathcal{C}(\rho)] \\ &= (-1)^{b_1} A \tilde{q}_0^m + [(-1)^{b_1+b_2} B_1 + (-1)^{b_2} B_2] \tilde{q}_1^m \\ &\quad + C, \end{aligned} \tag{22}$$

where

$$A := 2^{-1} \text{Tr}\left[E\mathcal{E}_{\mathcal{D}_j}(Z)\right] \text{Tr}(\rho Z), \tag{23}$$

$$B_1 := 2^{-1} \text{Tr}\left[E\mathcal{E}_{\mathcal{D}_j}(Y)\right] \text{Tr}(\rho Y), \tag{24}$$

$$B_2 := 2^{-1} \text{Tr}\left[E\mathcal{E}_{\mathcal{D}_j}(X)\right] \text{Tr}(\rho X), \tag{25}$$

$$C := 2^{-1} \text{Tr}\left[E\mathcal{E}_{\mathcal{D}_j}(\mathbb{I})\right]. \tag{26}$$

Equations (4)–(6) and (8)–(10) then follow from appropriate choices of b_1, b_2 and simple algebra.

Numerical simulation. Although the previous analysis is derived for gate- and time-independent noise, the randomized benchmarking protocol is both theoretically and practically robust to some level of gate-dependent noise [7,10]. We now illustrate through numerical simulations that this robustness holds for the dihedral benchmarking protocol, particularly in the regime where the noise is strongly gate dependent (as expected when the gates are implemented using different methods, namely, direct unitaries and magic-state injection).

For our simulations, each operation within the dihedral group $\mathcal{D}_8$ is generated by composing two gates, the first from $\mathcal{D}_4$ and the second is either identity or the $\pi/8$ gate. The error associated with the first gate is a simple depolarizing channel with an average fidelity of 0.9975. For the second gate, the error arises only after the $\pi/8$ gate, and corresponds to an over-rotation with an average fidelity of 0.99. The total average fidelity over $\mathcal{D}_8$ is 0.9925. Figure 2 shows the two decay curves described by Eqs. (5) and (6). Weighted nonlinear regressions give an estimate of 0.9924(1) for the average fidelity, which is consistent with the analytic value. We also simulate the interleaved randomized benchmarking protocol in two different regimes (see Fig. 3). The first regime [Fig. 3(a)] corresponds to over-rotation errors that are small for the Clifford operations, with average fidelity $1–10^{-6}$, but large

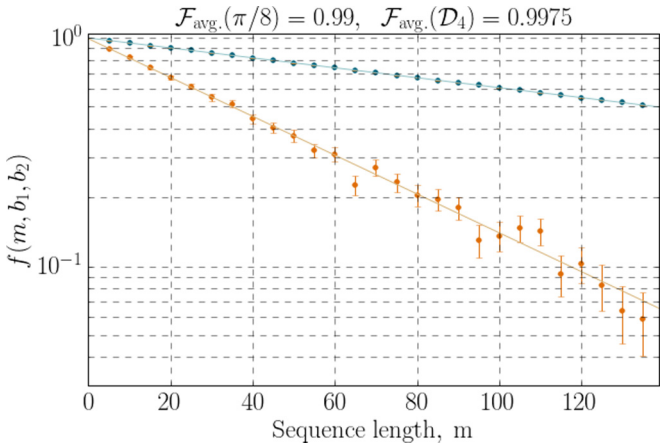

FIG. 2. (Color online) Decay curves corresponding to Eqs. (5) and (6) for a standard randomized benchmarking simulation with $A \approx \frac{1}{4}$ and $B \approx \frac{1}{2}$, respectively. The shallow (blue) and steep (orange) lines correspond to Eqs. (5) and (6), respectively. Each data point is obtained after averaging 500 sequences of fixed length. A weighted nonlinear regression (performed using the SCIPY Python package) gives an estimate of 0.9924(1) for the average fidelity over $\mathcal{D}_8$, compared to the analytic value 0.9925. See text for details.

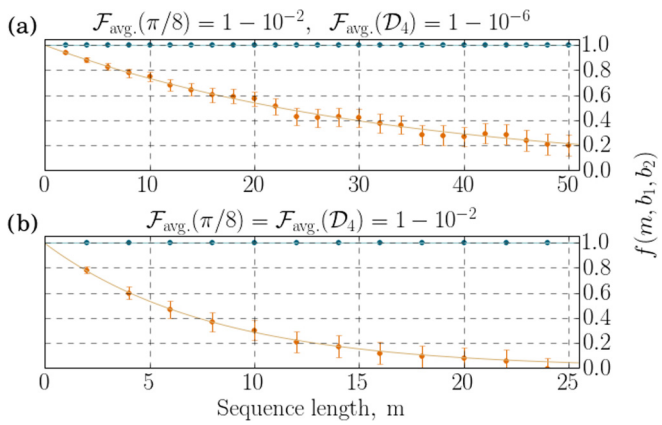

FIG. 3. (Color online) Decay curves corresponding to Eqs. (5) and (6) for an interleaved randomized benchmarking simulation with $A \approx \frac{1}{4}$ and $B \approx \frac{1}{2}$, respectively. The shallow (blue) and steep (orange) lines correspond to Eqs. (5) and (6), respectively. Each data point is obtained after averaging 500 sequences of fixed length. (a) corresponds to high-fidelity Clifford operations and a relatively noisy $\pi/8$ gate. (b) corresponds to errors of the same magnitude on the Clifford operations and the $\pi/8$ gate. See text for details.

for the $\pi/8$ gate, with average fidelity $1–10^{-2}$. The estimate of the fidelity of the $\pi/8$ gate via our protocol, 0.9901(2), is extremely precise in this regime. The second regime [Fig. 3(b)] corresponds to a similar over-rotation with average fidelity 0.99 both for the Clifford group and the $\pi/8$ gate. In this case the estimated value of $\mathcal{F}_{\text{avg}}(\mathcal{E}_{\pi/8})$ is 0.980 and the bound from Eq. (12) only guarantees $\mathcal{F}_{\text{avg}}(\mathcal{E}_{\pi/8})$ to lie in the interval $[0.958, 1.000]$. The rather loose bound in this regime is an open problem for interleaved randomized benchmarking and is not specific to the current protocol.

Conclusions. We have provided a protocol that extracts the average fidelity of the error arising over a group of single-qubit operations corresponding to the dihedral group. While we have explicitly assumed that the rotation axis is the z axis, this is an arbitrary choice. Since any single-qubit unitary can be written as a rotation about some axis on the Bloch sphere, our protocol can be used to characterize any single-qubit gate.

Of particular importance are $\mathcal{D}_8$ and $\mathcal{D}_4$, which enable efficient and precise benchmarking of the $\pi/8$ gate that plays a unique and important role in leading proposals for fault-tolerant quantum computation. We have illustrated numerically that the fidelity of the $\pi/8$ gate can be estimated using an interleaved version of our protocol. This estimate is precise when the quality of the Clifford gates is significantly greater than the $\pi/8$ gate, which is a regime relevant to near-term small-scale demonstrations of universal fault-tolerant quantum computation where Clifford operations are performed transversally while the quality of the $\pi/8$ gate is limited by the relatively high cost of magic-state distillation.

This research was supported by the U.S. Army Research Office through Grant No. W911NF-14-1-0103, CIFAR, the Government of Ontario, and the Government of Canada through NSERC and Industry Canada.

[1] I. L. Chuang and M. A. Nielsen, J. Mod. Opt. **44**, 2455 (1997).
[2] J. F. Poyatos, J. I. Cirac, and P. Zoller, Phys. Rev. Lett. **78**, 390 (1997).
[3] S. T. Merkel, J. M. Gambetta, J. A. Smolin, S. Poletto, A. D. Córcoles, B. R. Johnson, C. A. Ryan, and M. Steffen, Phys. Rev. A **87**, 062119 (2013).
[4] J. Emerson, R. Alicki, and K. Życzkowski, J. Opt. B: Quantum Semiclassical Opt. **7**, S347 (2005).
[5] E. Knill, D. Leibfried, R. Reichle, J. Britton, R. B. Blakestad, J. D. Jost, C. Langer, R. Ozeri, S. Seidelin, and D. J. Wineland, Phys. Rev. A **77**, 012307 (2008).
[6] E. Magesan, J. M. Gambetta, and J. Emerson, Phys. Rev. Lett. **106**, 180504 (2011).
[7] E. Magesan, J. M. Gambetta, and J. Emerson, Phys. Rev. A **85**, 042311 (2012).
[8] C. Dankert, R. Cleve, J. Emerson, and E. Livine, Phys. Rev. A **80**, 012304 (2009).
[9] D. Gottesman, Proc. Symp. Appl. Math. **68**, 13 (2010).
[10] J. J. Wallman and S. T. Flammia, New J. Phys. **16**, 103032 (2014).
[11] Y. R. Sanders, J. J. Wallman, and B. C. Sanders, arXiv:1501.04932 .
[12] D. Puzzuoli, C. Granade, H. Haas, B. Criger, E. Magesan, and D. G. Cory, Phys. Rev. A **89**, 022306 (2014).
[13] E. Magesan, D. Puzzuoli, C. E. Granade, and D. G. Cory, Phys. Rev. A **87**, 012324 (2013).
[14] M. Gutiérrez and K. R. Brown, Phys. Rev. A **91**, 022335 (2015).
[15] R. Barends, J. Kelly, A. Veitia, A. Megrant, A. G. Fowler, B. Campbell, Y. Chen, Z. Chen, B. Chiaro, A. Dunsworth, I.-C. Hoi, E. Jeffrey, C. Neill, P. J. J. O'Malley, J. Mutus, C. Quintana, P. Roushan, D. Sank, J. Wenner, T. C. White, A. N. Korotkov, A. N. Cleland, and J. M. Martinis, Phys. Rev. A **90**, 030303 (2014).
[16] S. Bravyi and A. Kitaev, Phys. Rev. A **71**, 022316 (2005).
[17] A. M. Meier, B. Eastin, and E. Knill, arXiv:1204.4221.
[18] S. Kimmel, M. P. da Silva, C. A. Ryan, B. R. Johnson, and T. Ohki, Phys. Rev. X **4**, 011050 (2014).
[19] E. Magesan, J. M. Gambetta, B. R. Johnson, C. A. Ryan, J. M. Chow, S. T. Merkel, M. P. da Silva, G. A. Keefe, M. B. Rothwell, T. A. Ohki, M. B. Ketchen, and M. Steffen, Phys. Rev. Lett. **109**, 080505 (2012).
[20] A. J. Landahl and C. Cesare, arXiv:1302.3240 .
[21] S. Forest, D. Gosset, V. Kliuchnikov, and D. McKinnon, J. Math. Phys. **56**, 082201 (2015).
[22] G. Duclos-Cianci and D. Poulin, Phys. Rev. A **91**, 042315 (2015).
[23] C. Granade, C. Ferrie, and D. G. Cory, New J. Phys. **17**, 013042 (2015).
[24] J. M. Gambetta, A. D. Córcoles, S. T. Merkel, B. R. Johnson, J. A. Smolin, J. M. Chow, C. A. Ryan, C. Rigetti, S. Poletto, T. A. Ohki, M. B. Ketchen, and M. Steffen, Phys. Rev. Lett. **109**, 240504 (2012).
[25] A. C. Dugas, J. Wallman, and J. Emerson (unpublished).
[26] A. G. Fowler, M. Mariantoni, J. M. Martinis, and A. N. Cleland, Phys. Rev. A **86**, 032324 (2012).
[27] M. A. Nielsen, Phys. Lett. A **303**, 249 (2002).